



HAL
open science

Gas adsorptive desulfurization of thiophene by spent coffee grounds-derived carbon optimized by response surface methodology: Isotherms and kinetics evaluation

Hiba Aouled Mhemed, Mylène Marin Gallego, Jean-François Largeau, Sana Kordoghli, Fethi Zagrouba, Mohand Tazerout

► To cite this version:

Hiba Aouled Mhemed, Mylène Marin Gallego, Jean-François Largeau, Sana Kordoghli, Fethi Zagrouba, et al.. Gas adsorptive desulfurization of thiophene by spent coffee grounds-derived carbon optimized by response surface methodology: Isotherms and kinetics evaluation. *Journal of Environmental Chemical Engineering*, 2020, 8 (5), pp.104036. 10.1016/j.jece.2020.104036 . hal-02881866

HAL Id: hal-02881866

<https://hal.science/hal-02881866>

Submitted on 13 Oct 2023

HAL is a multi-disciplinary open access archive for the deposit and dissemination of scientific research documents, whether they are published or not. The documents may come from teaching and research institutions in France or abroad, or from public or private research centers.

L'archive ouverte pluridisciplinaire **HAL**, est destinée au dépôt et à la diffusion de documents scientifiques de niveau recherche, publiés ou non, émanant des établissements d'enseignement et de recherche français ou étrangers, des laboratoires publics ou privés.

1 **Gas adsorptive desulfurization of thiophene by spent coffee grounds-derived carbon**
2 **optimized by response surface methodology: Isotherms and kinetics evaluation**

3 **Hiba Aouled Mhemed^{1,2,3}, Mylène Marin Gallego¹, Jean-François Largeau^{1,4}, Sana**
4 **Kordoghli³, Fethi Zagrouba², Mohand Tazerout¹**

5 [1] GEPEA- CNRS UMR 6144, IMT Atlantique, Nantes, 44000, France

6 [2] Research Laboratory for Sciences and Technologies of Environment LR16ES09, High
7 Institute of Sciences and Technologies of Environment, Borj Cedria, Carthage University,
8 Tunisia

9 [3] National School of Engineers of Gabes, University of Gabes, 6026 Gabes, Tunisia

10 [4] Icam, 35 rue du Champ de Manœuvres, 44430 Carquefou, France

11 **Corresponding author:** Mylène Marin Gallego, mylene.marin-gallego@imt-atlantique.fr, 4
12 rue Alfred Kastler BP20722 44307 Nantes Cedex 3 France.

13

14 **Abstract:**

15 **The elimination of sulfur compounds in the FCC gasoline is indispensable to protect**
16 **downstream equipment.** Researchers are trying to find technological innovations to produce
17 the famous “zero sulfur” fuel. Many adsorbents, such as spent coffee grounds-derived carbon
18 (SCG-AC), have been claimed to be effective in H₂S removal. However, no study has been
19 conducted to exploit its ability to eliminate the organo-sulfur compounds present **in FCC**
20 **gasoline** such as thiophene. This work involves the optimization by the response surface
21 methodology (RSM) of different operating conditions of activated carbon (AC) production by
22 the chemical activation (H₃PO₄) of SCG. RSM was used to estimate the variables considered
23 in the **preparation** of AC using the Box–Behnken Design (BBD). **The optimized SCG-AC was**
24 **used for the adsorption of thiophene through batch tests at ambient conditions.** The
25 equilibrium experimental data of the thiophene adsorption were analyzed by Langmuir,
26 Freundlich, and Langmuir–Freundlich isotherms. The adsorption isotherm data fit the
27 Langmuir–Freundlich isotherm **where the adsorption’s kinetics were described by the Elovich**
28 **model.** The optimum SCG-AC exhibited the highest adsorption capacity, with up to 2.23
29 mmol/g. **These results revealed that SCG-AC is a promising and economical adsorbent for the**
30 **elimination of thiophenic sulfur compounds.**

1 **Keywords:** spent coffee grounds-derived carbon (SCG-AC), RSM, thiophene, desulfurization

2 **Highlights**

- 3 • Activated carbon from spent coffee grounds (SCG-AC) was optimized through RSM.
- 4 • The adsorptive desulfurization of thiophene was investigated by SCG-AC.
- 5 • Thiophene removal from gas by SCG-AC was assessed at ambient conditions.
- 6 • The adsorption of thiophene via SCG-AC followed the Langmuir–Freundlich isotherm.
- 7 • The thiophene adsorption’s kinetic was described by the Elovich model.

8 **1. Introduction**

9 In the last two decades, environmental regulations to reduce sulfur in fuels have taken effect
10 [1]. Due to the European Commission and the Environmental Protection Agency (EPA)
11 reducing sulfur-containing organic compounds in fluidized catalytic cracking (FCC) gasoline
12 is required [2]. During the combustion of fuel, sulfur compounds can cause poisoning of the
13 catalyst [1], corrosion of downstream piping [3], and the release of SO_x. The literature have
14 studied sulfur compound elimination methods. Among the proposed methods,
15 hydrodesulfurization (HDS) is the current desulfurization method in use at oil refineries [4].
16 The HDS process has seen improvements in catalysis and process design [5]. The HDS
17 reaction varies depending on the different compounds that have sulfur and this lowers its
18 efficiency. HDS tends to be more effective when removing aliphatic sulfuric compounds such
19 as thiols, thioethers, sulfides, and disulfides; and it is less effective for thiophene and its
20 derivatives. This is explained by that their elimination requires much higher pressure and
21 temperature due to the steric hindrance of sulfur atoms [6]. HDS is not a cost-effective
22 operation because it requires severe operating conditions, i.e. high pressure and temperature,
23 and a further requirement like the excessive use of hydrogen and catalysts [1]. From this, the
24 HDS process is not cost-effective for the production of low to zero level sulfur [7].

1 Researchers have thought to develop alternative and more cost-effective HDS techniques.
2 Recently, processes that can be substituted for HDS have been developed. Examples of these
3 alternatives to HDS are as follows: shifting of boiling point by alkylation [8], desulfurization
4 via extraction by the transfer of sulfur from oil to solvents [9], desulfurization via oxidation
5 where the fuel is mixed with an oxidant compound followed by a separation of the formed
6 polar sulfones through extraction or adsorption [10], [8], sulphCo desulfurization where sulfur
7 compounds are oxidized in a water-fuel containing H₂O₂ catalyst via ultrasound [11], and the
8 oxidative desulfurization process employing photocatalysis where sulfur compounds can be
9 photo-oxidized to CO₂, SO₄²⁻, sulfoxides, and sulfones [12]. Among the proposed alternatives
10 to reduce sulfur levels, adsorptive desulfurization is the most attractive and cost-effective
11 method for removing organosulfur compounds because of low-energy consumption,
12 operational at ambient temperatures and pressures, the regeneration of consumed adsorbent,
13 and the availability of adsorbents [5]. Many adsorbents are commonly used for adsorptive
14 desulfurization, including zeolites [13] silica gel [14], and porous organometallic materials
15 (MOFs) [15]. Metal oxides (MnO, ZnO, and CaO) are also being researched [1]. Activated
16 carbons (ACs) have been studied as sulfur compound removal for different fuels [1], [3], [5],
17 [16], because they have a large surface area, well-developed porous structure, various surface
18 functional groups, high numbers of surface functional groups, a high degree of surface
19 reactivity, and good mechanical strength [17]. From this, precursor type, activating agent, and
20 preparation conditions significantly impact the texture and the chemical characteristics of AC
21 [5]. Traditionally, AC production optimization was conducted through the monitoring of one
22 factor to see its influence from the experimental response. Major issues using this technique
23 include a lack of interactive effects among the studied variables, the increase in the number of
24 experiments, time and consuming reagents and materials. To overcome this issue,
25 optimization was conducted using multivariate statistical techniques [18]. For the

1 optimization of the preparation process, Response Surface Methodology (RSM) has been
2 shown as an effective statistical tool [19]. It combines statistical and mathematical techniques
3 to develop, improve, and optimize processes [20]. This method builds a polynomial equation
4 based on experimental data to define the data set. The objective of this method is to assist
5 with statistical previsions. It is applicable when a response or a set of responses shows
6 influence from several variables. The literature has indicated that RSM is well applied to
7 optimize the production of AC from numerous precursors [21–24].

8 The selection of a proper adsorbent to eliminate sulfur compounds needs to consider the
9 following parameters like cost-effectiveness, availability, and adsorptive properties. Many
10 adsorbents were used in various adsorptive desulfurization studies. Many of them have
11 successfully retained sulfur compounds such as H₂S but failed to eliminate heterocyclic sulfur
12 compounds [3]. In this study, a cost-effective and sustainable material like spent coffee
13 grounds (SCG) makes a good precursor for the preparation of AC. The produced adsorbent
14 was then applied to adsorptive desulfurization. SCG residue is a good choice as an adsorbent
15 for the following reasons: its abundant production by the coffee industry; the production rate
16 goes as high as 748,000 tons per year [25]; and AC prepared from SCG has been proved to be
17 a good candidate for H₂S removal. One study revealed that the functional groups of nitrogen
18 present on the activated carbon derived spent coffee grounds surface have an important
19 catalytic role in the oxidation of hydrogen sulfide [26]. Nevertheless, no study has been
20 conducted to exploit its ability to eliminate heterocyclic sulfur compounds. As thiophene
21 compound exist in a great fraction of the entire sulfur content in FCC gasoline [27], the
22 proposed challenge was to prepare AC from SCG-AC and test its performance towards
23 thiophene removal as a heterocyclic sulfur compounds model present in FCC gasoline.

24 Activated carbons are commonly used for emission control at low concentrations. While the
25 adsorption of thiophene on AC is well known and researched for the deep desulfurization of

1 fuels in liquid phase [1,16,28], the literature is more scarce concerning the gas phase
 2 adsorption [3].
 3 **This research examined the systematic optimization of the activated carbon production**
 4 **from spent coffee grounds (SCG-AC), with phosphoric acid (H₃PO₄) activation and exploited**
 5 **its ability for thiophene removal from the gas phase at ambient conditions. To optimize the**
 6 **AC production process, the Box–Behnken design in the response surface methodology (RSM)**
 7 **was investigated. The following factors were chosen: acid concentration, impregnation ratio,**
 8 **and activation temperature for use in this study. Two responses including iodine number (IN)**
 9 **and methylene blue number (MB) were explored. IN and MB were selected for the**
 10 **measurement of micropore content and qualitative mesopore structure, respectively [5]. Since**
 11 **there is insufficient information on the kinetic and isotherm studies for gas-solid adsorption**
 12 **systems, kinetic and isotherm analysis of thiophene adsorption was discussed. Fig. 1 shows**
 13 **the experimental approach used in this study.**

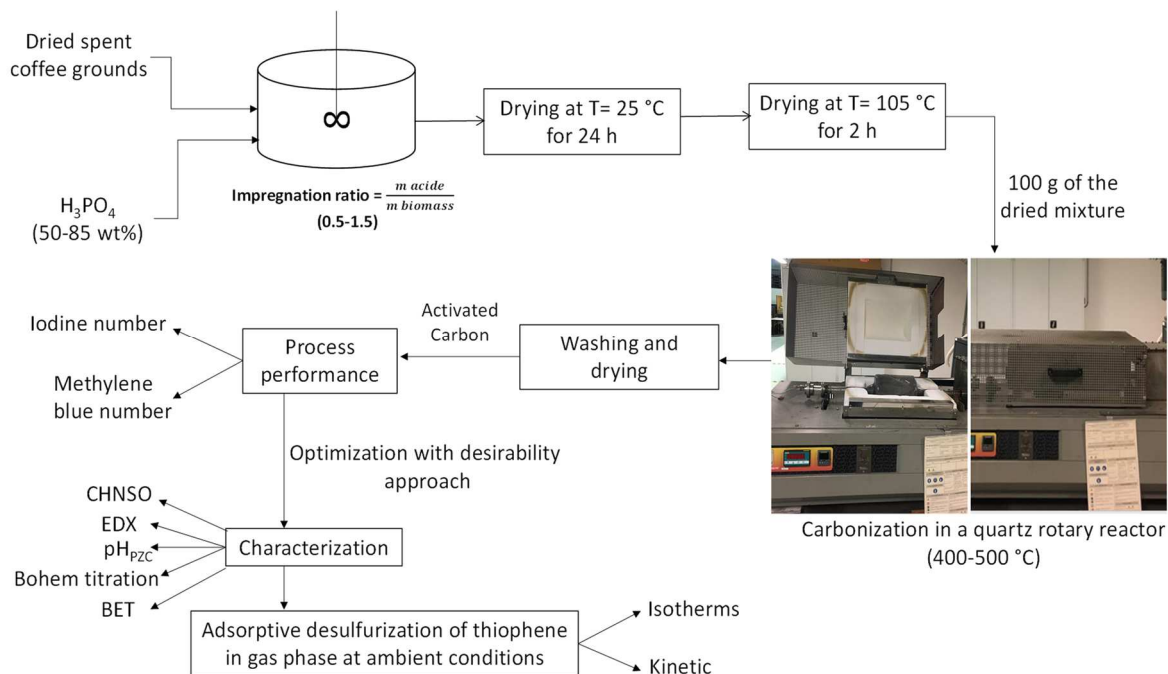


Fig. 1. Experimental process setup.

14
15

16 **2. Materials and Methods**

1 **2.1. Materials**

2 Spent coffee grounds used in this study was locally collected from the university cafeteria of
3 IMT Atlantique, Nantes (France). Phosphoric acid 85% (purity 98%), thiophene (purity 98%),
4 iodine (purity 99%), and methylene blue (technical quality) were purchased from Sigma-
5 Aldrich Co. Hydrochloric acid (purity 99.5%), Sodium Chloride (purity 99.5%), were
6 purchased from Acros Chemicals. Sodium hydroxide (analytical quality) was obtained from
7 Fischer Scientific.

8 **2.2. Preparation of the precursor and the activated carbon**

9 Samples of spent coffee grounds were first dried in an oven at 50 °C for 48 hours. A quantity
10 of 100 g of dried spent coffee grounds (SCG) was mixed with a solution of phosphoric acid
11 H₃PO₄ at different concentrations (85 wt%, 50 wt%, and 67.5 wt%). The impregnation ratio,
12 defined as the weight of impregnant (H₃PO₄)/weight of precursor (spent coffee grounds), was
13 0.5, 1 and 1.5. The mixture was left at room temperature for 24 h and then dried in an oven at
14 105 °C for 2 h. Then the mixture was introduced into a horizontal tubular furnace and heated
15 from room temperature to desired temperature (400-500 °C) at a heating rate of 5 °C.min⁻¹ for
16 120 min. The obtained products were cooled to room temperature inside the reactor in the
17 existence of a flow of nitrogen and then washed numerous times with distilled water until
18 neutralization of the pH of the rinse water. SCG-AC was finally dried at 105 °C for 24 h. The
19 steps of the activated carbon derived-spent coffee grounds production were presented in Fig.
20 1.

21 **2.3. Characterization of the SCG and SCG-AC**

22 Several analyses were performed to characterize the materials.

23 The proximate analysis of the precursor material (SCG) and SCG-AC (activated carbon
24 obtained on optimal conditions) were determined by a FLASH EA 1112 Series CHNS-O
25 analyzer (Thermo-finnigne instrument, Netherlands). The mineral matter content (EDX) was

1 measured using X-ray Fluorescence model EDX-800HS2 (Shimadzu, USA).
2 Thermogravimetric analysis (TGA) were carried out using a STSYS Evolution 1750
3 (SETARAM, France). For this analysis, 6 mg of powder samples were thermally treated
4 under an inert atmosphere of N₂ (20 ml/min) at 5 °C/min. The Sample was placed in an
5 alumina crucible and heated from room temperature to 800 °C to evaluate the thermal
6 decomposition of the lignocellulosic material and measure the mass loss.

7 In order to have a general look at the effect of the presence of phosphoric acid on the spent
8 coffee grounds pyrolysis process and compare it with the thermogravimetric results, two
9 experiments were performed. The first test consists on pyrolyzing the spent coffee grounds
10 (SCG) in the same conditions as the TGA in a rotary quartz reactor. The second experiment
11 was to add phosphoric acid to the SCG whilst preserving the same operating conditions as
12 before. In order to manipulate the gases produced during the pyrolysis process in these two
13 experiments, a Micro GC R-3000 (SRA INSTRUMENTS, France) was established at the
14 outlet of the horizontal rotary quartz reactor. The gas samples were taken automatically every
15 three minutes.

16 The micropore content of the SCG-AC was determined in terms of the iodine number (IN).
17 The iodine number was deduced due to the ASTM D4607-14 method [29]. The qualitative
18 mesopore structure of SCG-AC was evaluated by methylene blue (MB) adsorption at room
19 temperature. The MB concentration was calculated using a JENWAY6300 UV-Vis
20 spectrophotometer at a maximum wavelength of 665 nm [29].

21 The textural properties of optimal SCG-AC were determined by N₂ adsorption at 77 K using
22 Micromeritics Smart VacPrep. The surface area (S_{BET}) of the optimal SCG-AC was measured
23 with a surface area analyzer. The total pore volume was deduced from the quantity of nitrogen
24 adsorbed at P/P^o = 0.95, by applying the Barret-Joiner-Halenda method (BJH) [17].

1 The point of zero charge pH_{pzc} characterizes the charge at the surface of the SCG-AC. If $pH >$
2 pH_{pzc} the adsorbent has a negative surface charge. If $pH < pH_{pzc}$ the adsorbent has a positive
3 **surface charge**. It is defined as the pH of the aqueous solution in which the solid exists under
4 a neutral electrical potential. Various pH solutions ranging from 2 to 10 were prepared by
5 mixing 0.1 g of activated carbon with 20 ml of 0.1M NaCl solution. The pH value was
6 adjusted by adding an aqueous solution of NaOH or HCl [30]. The acidic and basic functional
7 groups on the surface of the optimal SCG-AC were checked by Boehm's titration method
8 [31].
9 All analyzes were performed in three replicates.

10 **2.4. Design of experiments**

11 The SCG-derived carbon production **was** studied with the Response Surface Methodology
12 using the Box Behnken Design (BBD). **BBD requires three levels for each factor** [20]. The
13 variables studied were acid concentration (A), impregnation ratio (B) and activation
14 temperature (C). These three variables with their corresponding ranges were selected based on
15 the literature and preliminary studies [30].

16 The goal of the experimental design is to obtain a relation $y = f(x_i)$ between the response of
17 the system and the factors x_i . The interest of modeling the response by a polynomial equation
18 is to predict all the answers of the field of study, with a limited number of experiments. **The**
19 **different levels for each process variable (low, middle and high levels) were designated as -1,**
20 **0 and +1, which led to 17 experimental runs. Replication at the center points was applied to**
21 **estimate experimental errors**. The experimental design chosen involved three-level and three-
22 factors. **The work domain coding for these three factors is presented in Table 1.**

23 In our case, the mathematical model is a polynomial model of second order, which takes into
24 account the main effects β_i and the interactions β_{ii} and β_{ij} . The equation $y = f(x_i)$ will be
25 written as [17]:

$$y = \beta_0 + \sum_{i=1}^n \beta_i x_i + \sum_{i=1}^n \beta_{ii} x_i^2 + \sum_{i=1}^{n-1} \sum_{j=i+1}^n \beta_{ij} x_i x_j \quad (1)$$

1 Where β_0 is the coefficient of intercept. β_i , β_{ii} and β_{ij} are the linear, quadratic and interaction
2 coefficients respectively; x_i are the coded variables.

3 Expert design 11.0.1.0 (Stat-Ease, Minneapolis, USA) was used for the statistical analysis of
4 the experimental data. The quality of the fit of the polynomial model was expressed by the
5 correlation coefficient (R^2). The significance and adequacy of the used model was further
6 explained using F-value (Fisher variation ratio), probability value (Prob > F), and adequate
7 precision (AP) [32].

8 **Table 1. Association of factors with coded variables in the experimental design**

Factor	Code	Units	Coded variable level		
			-1	0	+1
Acid concentration (A)	A	wt%	50	67.5	85
Impregnation ratio (B)	B	g/g	1:2	1:1	1.5 :1
Activation temperature (C)	C	°C	400	450	500

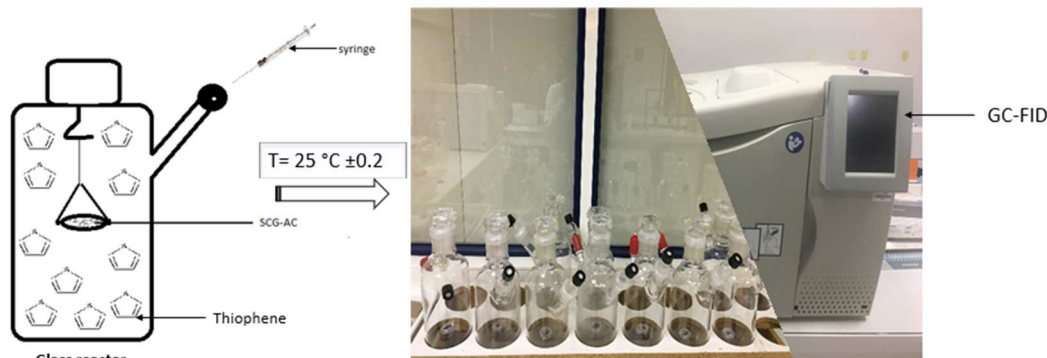
9 **2.5. Adsorption of sulfur compound**

10 The optimum SCG-derived carbon (from RSM) was dried in an oven at 105 °C for 2 hours
11 before use. A common isotherm method was applied. Fixed known weighed amounts of the
12 SCG-AC were suspended in identical batch reactors of 2 liters (see Fig. 2). Different weighed
13 amounts of liquid thiophene were added and volatilized. The thiophene's initial concentration
14 was kept lower than the saturating vapor pressure to avoid condensation in the reactors. The
15 volumes injected vary between 20 and 300 μ l at 25 °C \pm 0.2 °C for 500 min. Once
16 equilibrium was reached, the remaining pollutant concentration was measured by gas
17 chromatograph (Chromatography Perkin Elmer Clarus 500) equipped with a flame
18 photometric detector. To study the adsorption kinetics on the SCG-AC, 100 ppm of thiophene
19 was injected in the batch reactor and was controlled until equilibrium is reached.

20 The amount of adsorbed thiophene is calculated using the following equation:

$$qe = \frac{(C_0 - C_e) \cdot V}{m} \quad (2)$$

1 Where q_e : amount of solute adsorbed at equilibrium per unit weight of adsorbent (mmol/g);
 2 C_e : thiophene concentration at equilibrium (mmol/l); m : mass of adsorbent (g); C_0 : initial
 3 concentration of thiophene (mmol/l); V : volume of the reactor (l).



4
5 **Fig. 2. Adsorption experiments**

6 The removal efficiency of the SCG-AC was evaluated using the following mathematical
 7 equation:

$$\% \text{ Adsorption} = \frac{C_i - C_e}{C_i} \times 100 \quad (3)$$

8 where C_i (ppm): initial adsorbate (thiophene) concentration and C_e (ppm): equilibrium
 9 adsorbate concentration.

10 **2.5.1. Adsorption isotherms**

11 Different models have been used in the literature to describe the adsorption isotherms. The
 12 Langmuir, Freundlich, and Langmuir–Freundlich models are the most frequently used models
 13 for the adsorption process. In this work, we used these isotherm models to fit the experimental
 14 data for the adsorption of thiophene from gas phase onto the SCG-AC at ambient conditions.

15 The Langmuir isotherm is [33]:

$$q_e = \frac{q_m K_L C_e}{1 + K_L C_e} \quad (4)$$

16 Where q_m is the saturation value of q_e and K_L is the Langmuir constant. In this model, it is
 17 assumed that the number of adsorption sites on the surface of the AC is fixed and that each
 18 site can adsorb only one particle. This model neglects the interaction between adsorbed
 19 particles [34].

1 The Freundlich isotherm is:

$$q_e = K_F C_e^{\frac{1}{n}} \quad (5)$$

2 Where K_F and $1/n$ are the Freundlich constants. Freundlich model can be applied in many
3 cases, especially in the case of multilayer adsorption with possible interactions between the
4 adsorbed molecules at low concentrations. Although its accuracy, this model has the
5 disadvantage of not providing an upper limit to the solid phase concentrations [5].

6 The Langmuir–Freundlich isotherm is [35]:

$$q_e = \frac{q_m (K_{LF} C_e)^{\frac{1}{n}}}{1 + (K_{LF} C_e)^{\frac{1}{n}}} \quad (6)$$

7 Where K_{LF} and n are constants. The value of n indicates the heterogeneity of the site energies.

8 The Langmuir-Freundlich is able to model the distribution adsorption isotherm of an
9 adsorbate at high and low concentrations [36].

10 **2.5.2. Kinetic models**

11 The adsorption kinetic of thiophene was investigated using three model: the pseudo-first
12 order, pseudo-second order, and the Elovich model.

13 The pseudo-first-order kinetic model is mainly used to describe the initial stages of the
14 adsorption process [37]. It is defined according to the Lagergren's (1898) relation by:

$$\ln(q_e - q_t) = \ln q_e - K_1 \times t \quad (7)$$

15 Where, q_e (mmol/g) and q_t (mmol/g) are the amounts of adsorbed thiophene at equilibrium
16 and time t (min), respectively; k_1 (min^{-1}) is the rate constant of the Lagergren-first-order
17 kinetics model.

18 The pseudo-second-order model is based on the assumption that the limiting stage of the
19 reaction rate can be the chemisorption involving valence forces by electron exchange between
20 the adsorbent and the adsorbate [37]. The equation of the psudo-second-order model is
21 defined by [38]:

$$\frac{t}{q_t} = \frac{1}{K_2 q_e^2} + \frac{t}{q_e} \quad (8)$$

1 Where q_t is the amount of thiophene (mmol/g) at a time (min) and k_2 (g/(mmol min)) is the
2 adsorption rate constant.

3 Elovich model is introduced to further study the adsorption process. Elovich model is one of
4 the most often used models to describe chemisorption kinetics. It is also successfully applied
5 to describe the initial adsorption step and multilayer adsorption on a high heterogeneous
6 surface area [33].

$$q_t = \left(\frac{1}{\beta}\right) \ln(\alpha \times \beta) - \left(\frac{1}{\beta}\right) \ln(t) \quad (9)$$

7 where α is equilibrium rate constant, $\text{mmol g}^{-1} \text{min}^{-1}$, and β is a constant referred to
8 surface coverage and activation energy of chemisorption, g.mmol^{-1} . In the case when the
9 correlation between the adsorption capacity and the constant β is negative it is assumed that
10 the adsorbent does not retain the adsorbate.

11 **2.5.3. Adsorption mechanism**

12 The kinetic experimental results were also applied to the Weber intraparticle diffusion
13 mechanism to include the stages touching the adsorption kinetics. The equation is defined by
14 Weber and J.C [39]:

$$q_t = K_{id} t^{0.5} + C \quad (10)$$

15 Where C is the intercept (mmol/g) which is related to the boundary layer thickness and k_{id} is
16 the slope which represents the intraparticle diffusion rate constant ($\text{mmol/g min}^{1/2}$).

17 **3. Results and discussion**

18 **3.1. Characterization of the precursor (SCG) and the influence of the active agent**

19 **(H₃PO₄)**

20 Table 2 shows both proximate and ultimate analysis of raw material. SCG contained a good
21 percentage of carbon (50.40 wt%) and oxygen (38.50 wt%). This could be due to the higher
22 lignin contents in the spent coffee grounds. However, ultimate analysis showed a high levels

1 of nitrogen (~2.40 wt%) in the studied precursor, certainly due to its high protein content [40].
 2 The elemental analysis of the SCG showed a low ash content of 1.8 % with a volatile content
 3 of 77.90 wt% hence a lower fixed carbon content (20.3 wt%). The basic elemental
 4 constituents of biomass minerals are Si, Ca, K, and Mg with smaller amounts of S, P, Fe, and
 5 Cu. The existence of inorganic minerals, especially the alkali (K, Na, etc.) and alkaline-earth
 6 metals (Mg, Ca, etc.) influence the biomass pyrolysis mechanism. For example, K in the
 7 biomass mineral matter catalytically favors char formation [41]. In our case, spent coffee
 8 grounds contains a high percentage in K; therefore, it is suitable for char production.
 9 Contrariwise biomass with high percentages of alkali metals and Cl are less desirable as fuel
 10 because it causes fouling, deposition, corrosion, plugging, and agglomeration [42]. According
 11 to the EDX analysis the amount of alkali metals and Cl in spent coffee grounds is low (less
 12 than 10 wt%).

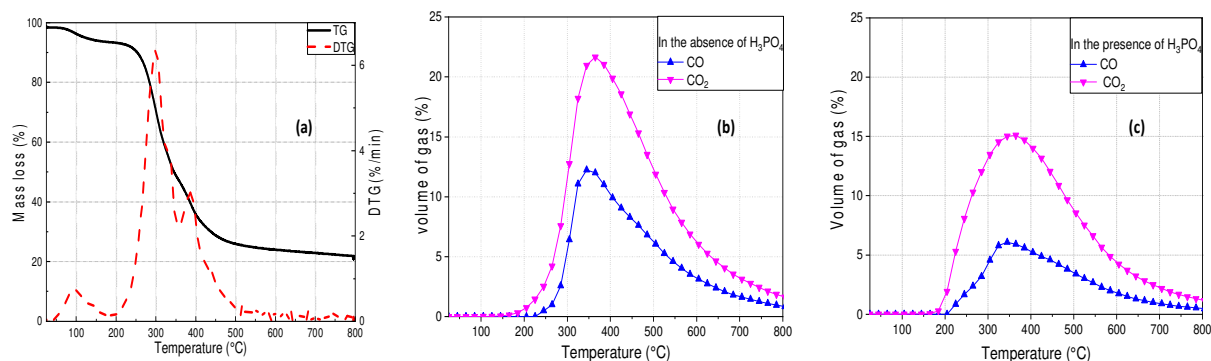
13 **Table 2. Proximate and ultimate analysis of the raw material**

Ultimate analysis (wt%)				
C	H	N	S	O*
50.40	6.90	2.40	<0.06	38.50
Proximate analysis (wt%)				
Volatils yields ^{db}		Fixed carbon	Ash	
77.90		20.30	1.80	
EDX analysis (wt%)				
K	Cl	Ca	P	Fe
0.76	2.10	1.23	0.046	0.05

14 *Obtained by difference
 15 ^{db} dry basis

16 The thermogravimetric analysis (TGA) of the SCG was conducted in absence of H₃PO₄ and is
 17 presented in the Fig. 3a. Additionally, pyrolysis experiments involving SCG were done on a
 18 large scale in a rotary reactor with both the presence and the absence of the activating agent
 19 H₃PO₄ (Fig. 3b and Fig. 3c). During the pyrolysis experiments in the rotary reactor the CO
 20 and CO₂ content of the pyrolysis gases were followed by micro-GC analysis. The results
 21 identified the optimal pyrolysis temperature and defined the decomposition scheme of the

1 functional groups on the surface of the SCG-AC. Weight loss occurred when the temperature
2 was between 25–150 °C and represents water evaporation. Mass loss occurred between 150–
3 450 °C and is characterized by the decomposition of hemicellulose and cellulose; and the
4 desorption of CO₂ and some CO (Fig. 3(a,b)). This phenomenon is described as the
5 decomposition of the following: carboxyl, lactone, and lactol groups [43]. When the
6 temperature is above 400 °C, then lignin decomposition and CO desorption occur (Fig. 3 b).
7 Desorption is caused by the decomposition of the following: carbonyl, ether, quinine, and
8 phenol groups on carbon surface. One study revealed that the rise of the release of the CO, in
9 the decomposition process, means the relative richness of carbonyl and phenol groups on the
10 surface of the synthesized AC [37]. The CO is primarily decomposed on temperatures above
11 600 °C. Phosphoric acid (H₃PO₄) when used as an activating agent (Fig. 3c) will lower
12 desorption of CO₂ on the AC surface, which led to the growth in the number of carboxylic
13 and lactonic groups. Further H₃PO₄ mitigates and forces the percentage by volume of CO
14 released from 12 to 6% which is considered an important reduction of the carbonyl and
15 phenol groups on the surface of AC. So our activated carbon prepared in temperature ranging
16 from 400 to 500 °C must be richer in carboxylic and lactonic functions than in carbonyl and
17 phenol functions. The hypothesis of this research has been proven from the results of Boehm
18 titration.



19
20 **Fig. 3. TGA analysis (a) and Micro-GC analysis of SCG pyrolysis without phosphoric**
21 **acid (b) and with phosphoric acid (c)**

3.2. Experimental results of the Design of experiments (DOE)

The experimental results obtained at the designed experimental conditions according to the Box Behnken design are presented in Table 3. From this table, we noticed that the SCG-AC sample activated at 400 °C in an acid concentration of 67.5 wt% with an impregnation ratio of 1.5 g/g gives the optimum iodine adsorption value (1133 mg/g). The greater methylene blue number of 93 mg/g is obtained by the activated carbon prepared at 500 °C in an acid concentration of 85 wt% with an impregnation ratio of 1 g/g. According to this table the relative error between the experimental and the predicted values is less than 5 %.

3.3. Statistical analysis

The analysis of variance (ANOVA) established the model of this research as well as to identify the relationship among the variables and the responses [24]. Table 4 lists the ANOVA for the quadratic models of the iodine number (IN) and methylene blue number (MB) responses. The significance of each parameter and interaction between different parameters is evaluated considering p-value and F-value. Commonly, large F-value and small p-value would prove the statistical implication of the model and the model terms. An, F-value and p-value > F were used to verify the significance levels for each coefficient used in this research [17]. Typically, if a value “Prob > F” is less than 0.05, then the terms of models are significant. For this research, all F-values are equal to 242.28, and 73.77 for IN and MB responses, respectively; and the Prob > F less than 0.0001 shows that the models used in this research are significant.

3.3.1. Iodine number (IN)

According to the ANOVA analysis for the iodine number, the substantial model terms for iodine adsorption are the acid concentration (A), impregnation ratio (B), interaction between acid concentration and impregnation ratio (AB), interaction between impregnation ratio and temperature (BC) and quadratic term of the primary factors of interest in the experiment A^2 ,

1 B^2 , and C^2 . The equation below (11) indicates the quadratic regression model that is defined
2 by all coded factors once all insignificant terms are excluded:

$$\text{Iodine number } \left(\frac{\text{mg}}{\text{g}}\right) = 1119 + 11.75 \times A + 19.12 \times B - 16.25 \times A \times B + \quad (11)$$
$$7.50 \times B \times C - 40.75 \times A^2 - 5.50 \times B^2 + 8 \times C^2$$

3 The acid concentration, impregnation ratio, and interaction between activation temperature
4 and impregnation ratio exhibited a positive impact on the iodine adsorption response.
5 However, the activation temperature is the only quadratic term that presented a positive
6 incidence on the iodine number. According to Table 4, we noticed that the impregnation ratio
7 has the most obvious effect on the iodine number based on the highest F-value of 398.69.
8 Hence, it could be perceived that the number of micropores were developed with the
9 impregnation ratio of 1.5 g/g in the studied domain. In fact, at the high level of the significant
10 model terms, the activation reaction may take place rapidly producing a development of
11 porosity of the obtained activated carbons and an increase in the microporosity [44].

12 3.3.2. Methylene blue number (MB)

13 The greatest important effects on the methylene blue adsorption are the three primary factors,
14 interaction between acid concentration and activation temperature (AB), interaction between
15 impregnation ratio and activation temperature (BC) and the quadratic term of the primary
16 factors of interest in the research A^2 , B^2 , and C^2 (see eq. 12).

$$\text{Methylene blue number } \left(\frac{\text{mg}}{\text{g}}\right) = 48 + 5.38 \times A - 5.56 \times B + 9.81 \times C + \quad (12)$$
$$12.75 \times A \times C + 4.88 \times B \times C - 4.06 \times A^2 + 7.06 \times B^2 + 20.31 \times C^2$$

17 The positive factor coefficients were indicators of a synergistic effects and negative factor
18 coefficients showed an antagonistic effect on these responses. The acid concentration,
19 activation temperature, interaction between acid concentration and activation temperature,
20 interaction between impregnation ratio and activation temperature presented a positive effect
21 on the MB response. Although, the quadratic term of the acid concentration showed a
22 negative effect on the expansion of mesopores. According to Table 4, among the primary

1 factors of interest the activation temperature has the most important effect on the methylene
2 blue number due to the higher F-value (99.33). Hence, the number of mesopores are
3 developed with the activation temperature of 500 °C in the studied field.

4 **3.4. Diagnostic model**

5 An equation's fitness is apparent from correlation coefficient, adequate precision and standard
6 deviation. The following values all indicate the responses are well correlated by the quadratic
7 model: Equation (11) showed correlation coefficient of ($R^2= 0.9877$); and equation (12)
8 showed correlation coefficient of ($R^2= 0.9917$). Adequate precision is a signal-to-noise ratio.
9 It compares the range of the predicted values at the design points to the average prediction
10 error. A value greater than 4 is desirable in support of the fitness of the model. The ratio of
11 43.95 and 25.86 for iodine number and methylene blue number respectively are greater than 4
12 which indicate an adequate signal. These models can be used to navigate the design space
13 [10]. Standard deviation used in this study were equal to 2.21 and 2.27 for equations (11) and
14 (12), respectively. A good capability for the developed quadratic models in this study has
15 been shown [17]. To signify the model's replicability, the variance coefficient (VC) was
16 developed from the ratio of standard error for estimates of the average value of the observed
17 responses. A model is considered replicable when the VC value is less than 10 % [17]. Both
18 models used in this research were shown to be replicable because both regressions ($VC1 =$
19 0.20% and $VC2 = 4.00 \%$) were less than 10 %.

1

Table 3. Independent variables and results for the preparation of activated carbon by the BOX-Behnken Design (BBD)

Run order	Acid Concentration (wt%)	Impregnation Ratio (g/g)	Temperature (°C)	Iodine number (mg/g)		Error, %	Methylene blue number (mg/g)		Error, %
				Actual	Predicted		Actual	Predicted	
1	67.5	0.5	500	1095.00	1095.75	0.07	83.00	85.87	3.46
2	67.5	1.0	450	1119.00	1119.00	0.00	48.00	48.00	0.00
3	85.0	0.5	450	1080.00	1081.63	0.15	63.00	60.94	3.27
4	85.0	1.0	400	1101.00	1099.38	0.15	46.00	47.06	2.30
5	50.0	1.5	450	1098.00	1096.38	0.15	37.00	38.06	2.86
6	50.0	1.0	400	1069.00	1071.38	0.22	61.00	61.81	1.33
7	67.5	1.0	450	1119.00	1119.00	0.00	48.00	48.00	0.00
8	67.5	1.0	450	1119.00	1119.00	0.00	48.00	48.00	0.00
9	50.0	0.5	450	1028.00	1025.63	0.23	53.00	52.19	1.53
10	50.0	1.0	500	1076.00	1077.63	0.15	58.00	55.94	3.55
11	67.5	1.0	450	1119.00	1119.00	0.00	48.00	48.00	0.00
12	85.0	1.0	500	1099.00	1096.63	0.22	93.00	92.19	0.87
13	67.5	1.0	450	1119.00	1119.00	0.00	48.00	48.00	0.00
14	67.5	0.5	400	1109.00	1109.00	0.00	76.00	76.00	0.00
15	85.0	1.5	450	1085.00	1087.38	0.22	51.00	51.81	1.59
16	67.5	1.0	450	1119.00	1119.00	0.00	48.00	48.00	0.00
17	67.5	1.5	400	1133.00	1132.25	0.07	57.00	55.12	3.30

1

Table 4. ANOVA results

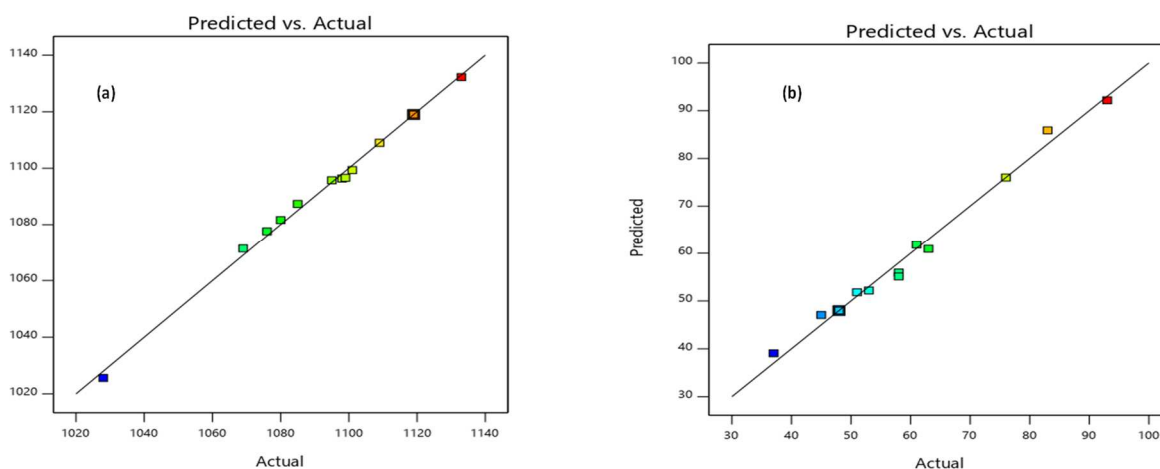
Source	ANOVA of IN						ANOVA of MB					
	Sum of Squares	df	Mean Square	F Value	p-value	Significance	Sum of Squares	df	Mean Square	F Value	p-value	Significance
Model	10668.81	9	1185.42	242.28	< 0.0001	Globally significant	3432.28	9	381.36	73.77	< 0.0001	Globally significant
A-Acid Concentration	1104.50	1	1104.50	225.74	< 0.0001	significant	231.13	1	231.13	44.71	0.0003	significant
B-Impregnation ratio	1950.75	1	1950.75	398.69	< 0.0001	significant	165.02	1	165.02	31.92	0.0008	significant
C-Activation temperature	4.08	1	4.08	0.83	0.3913	Not significant	513.52	1	513.52	99.33	< 0.0001	significant
AB	1056.25	1	1056.25	215.88	< 0.0001	significant	4.00	1	4.00	0.77	0.4082	Not significant
AC	20.25	1	20.25	4.14	0.0814	Not significant	650.25	1	650.25	125.78	< 0.0001	significant
BC	112.50	1	112.50	22.99	0.0020	significant	47.53	1	47.53	9.19	0.0191	significant
A²	5693.36	1	5693.36	1163.61	< 0.0001	significant	56.58	1	56.58	10.95	0.0130	significant
B²	103.71	1	103.71	21.20	0.0025	significant	171.01	1	171.01	33.08	0.0007	significant
C²	219.43	1	219.43	44.85	0.0003	significant	1414.62	1	1414.62	273.64	< 0.0001	significant
Residual	34.25	7	4.89				36.19	7	5.17			
Lack of Fit	34.25	2	17.13				36.19	2	18.09			
Pure Error	0.000	5	0.000				0.000	5	0.000			
Cor Total	10703.06	16					3468.47	16				

2

A: Acid concentration; B: Impregnation ratio; C: Activation temperature

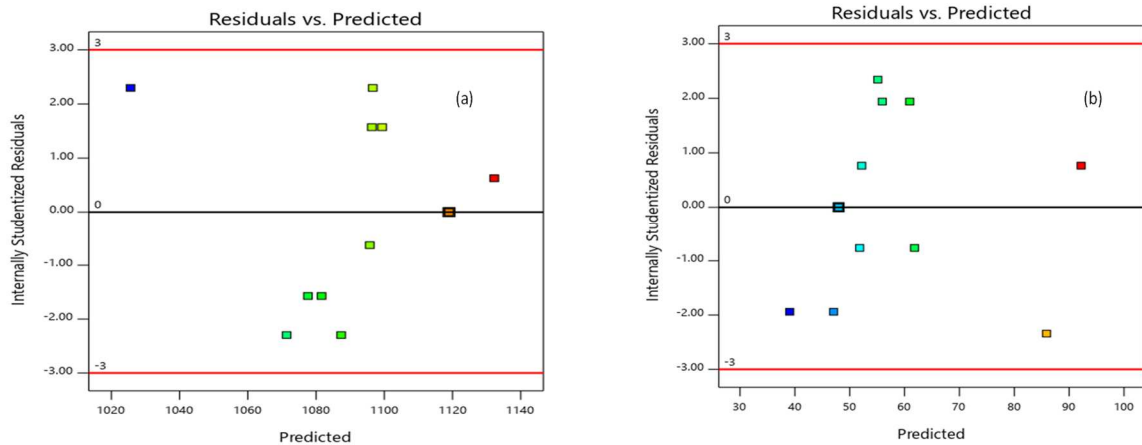
1 3.5. Evaluation of the model's plots

2 Fig. 4(a,b) represents the actual values versus the predicted values for iodine number and
3 methylene blue number responses, respectively. From those plots, most of the data points
4 were well dispersed near to the straight line. This is explicated by an excellent relationship
5 between the experimental and predicted values of the responses. Thus, these statistical tests
6 showed that the developed quadratic models could successfully correlate between the
7 variables of AC production and responses.



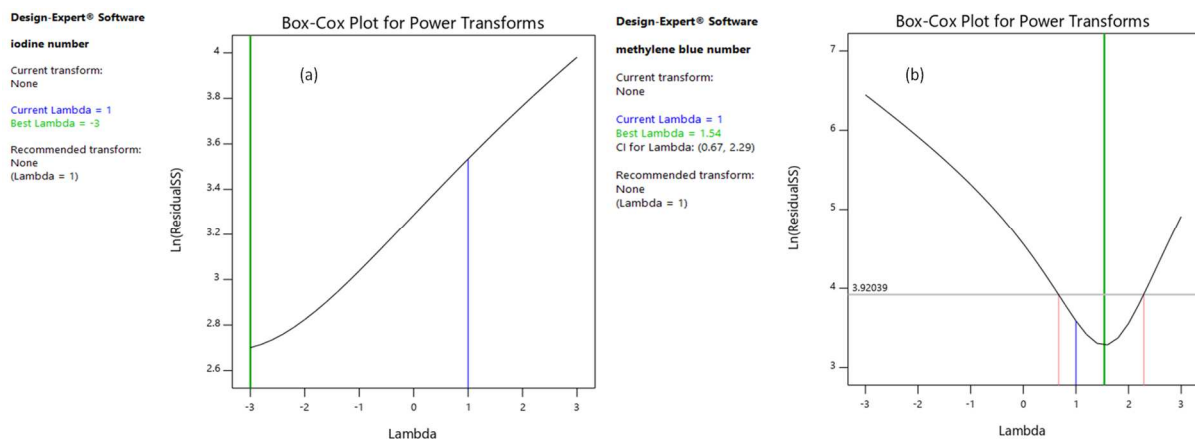
8 **Fig. 4. The experimental data versus predicted value plot for the (a) IN and (b) MB**
9
10 **responses.**

11 Fig. 5(a,b) shows the residual values versus predicted responses values for methylene blue
12 number and iodine number, respectively. By definition, the residual values signify the
13 difference between the actual and predicted response values. According to figure 5, we
14 noticed that the points have a random distribution for the two responses. The residuals are
15 located in a horizontal curve and the number of points that exist at the top and bottom of the
16 horizontal line is equal. In addition, the residual values are between ± 3.00 [45]. These results
17 confirm the validity of the proposed correlation.



1
2 **Fig. 5. The residuals data versus predicted value plot for the model (a) IN and (b) MB**
3 **responses.**

4 The Design-Expert software provides a diagnostic of the Box-Cox plot (see Fig. 6). This plot
5 provides a guideline for selecting the correct power law transformation by the choice of a
6 suitable λ value. The best value for λ is that corresponding to the minimum value for \ln
7 residual SS. This value is bounded by upper and lower 95 % confidence interval. If the 95 %
8 confidence interval around this λ includes 1 then no specific transformation is recommended.
9 Fig. 6(a,b) represent the Box-Cox plot for iodine and methylene blue number transformation,
10 respectively. We noticed that a 95 % confidence interval around the minimum point of the
11 curve contains 1. So, no specific transformation is recommended for the two models.



12
13 **Fig.6. Box-Cox plot for the model (a) IN (b) MB responses.**

1 **3.6. Interaction effects on the responses**

2 The contour plots were illustrated using Design-Expert® software, by varying two parameters
3 and keeping the other variable constant at the “zero” level. Fig. 7a shows the contour plot of
4 the combined effect of acid concentration (A) and impregnation ratio (B) on the iodine
5 number response at constant temperature (450 °C). The impregnation ratio defined as the
6 amount of phosphorous incorporated into the precursor is a parameter that controls the
7 development of the microporosity as well as the mesoporosity in the produced adsorbent [46].
8 The outline illustrates that both variables have a significant effect on the iodine number. A
9 maximum iodine number of about 1120 mg.g⁻¹ was attained with an impregnation ratio of
10 1.50 g/g and an acid concentration of 68.7 wt%. A further increase in the acid concentration
11 and the level of impregnation ratio leads to a considerable reduction in the adsorption of
12 iodine molecules. This can be explained by the production of heterogeneity on the micropore
13 size and later a mesoporosity of the SCG-AC.

14 Fig. 7b illustrates the shared effect of the impregnation ratio (B) and the activation
15 temperature (C) on the iodine number. The acid concentration is set at zero levels (A = 67.5
16 wt%). The adsorption of iodine increases from 1100 to 1140 mg/g with the increment of the
17 impregnation ratio from 0.5 to 1.5 g/g and temperature from 400 to 500 °C. A possible
18 explication for this phenomenon is that an increase of temperature can raise the degree of the
19 reaction H₃PO₄-precursor, thus resulting in increasing devolatilization, the development of the
20 pore structure, and the formation of a large number of active sites. Md-Desa et al.[47]
21 reported similar observations using AC from spent mushroom farming.

22 Fig. 7c illustrates the significant common interaction between acid concentration (A) and
23 activation temperature (C) on the methylene blue number at constant impregnation ratio (B =
24 1 g/g). The adsorption of methylene blue is improved when acid concentration increased to
25 reach a maximum adsorption value of 80 mg. g⁻¹. From the contour curve, it was noted that

1 when the temperature increased from 400 to 500 °C, the MB is enhanced by 33.33 %. Thus,
 2 the aromatic condensation reaction between adjacent molecules supports the development of
 3 the porous structure. Hence due to a higher temperature, the number of micropores decreases
 4 compared to the mesopores [19].

5 Fig. 7d illustrates the surface plot of MB adsorption as a function of impregnation ratio and
 6 activation temperature. From the plot, it is obvious that the MB adsorption increased with the
 7 increase in temperature from 440 to 500 °C and impregnation ratio from 0.8 to 1.5 g/g. The
 8 curve segment of the plot indicated that the MB adsorption was particularly touched by the
 9 interactive effects of impregnation ratio and activation temperature. The highest methylene
 10 blue number was reached at 500 °C and an impregnation rate of 1.5 g/g.

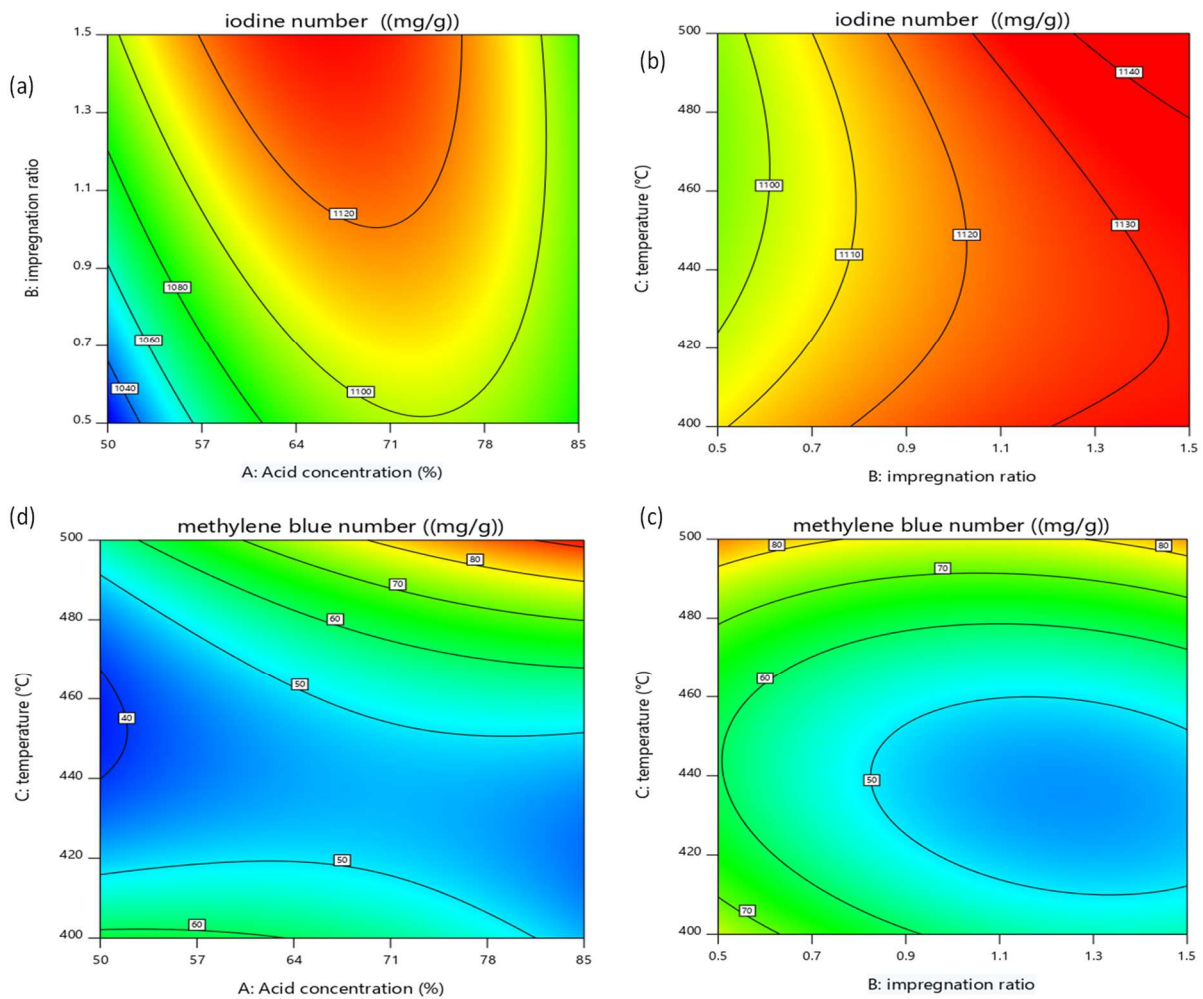


Fig.7. Contour plots of IN and MB responses

11
 12

1 **3.7. Process optimization**

2 This study purposes to control the optimal conditions to obtain an SCG-AC with a high
3 content of both mesopores and micropores. In order to find a compromise between the
4 adsorption of iodine and the methylene blue, the desirability function was applied using the
5 Expert Design software. **Box-Behnken design had been applied with the desirability approach**
6 **in order to optimize the preparation of activated carbon from SCG where the responses such**
7 **as iodine and methylene blue adsorption value were desired to be maximum** [19]. In this
8 optimization analysis, the operational variables were selected to remain within the value
9 range. The most suitable experimental conditions were selected for verification. Thus, the
10 optimal conditions of the SCG-AC preparation were: an activation temperature of 500 °C, an
11 acid concentration of 68.7 wt% and an impregnation ratio of 1.50 g/g with predictive values
12 for the number of iodine and methylene blue of 1148 mg.g⁻¹ and 86 mg.g⁻¹ respectively. The
13 experimental values obtained for the adsorption of iodine and methylene blue are in good
14 agreement with the predicted one (see Table 5). The relative low error percentage (< 5 %)
15 between the experimental and predicted values indicates the accuracy of the optimization
16 process. According to the literature, the adsorption capacity of an adsorbent is related to its
17 adsorption capacity for smaller nonpolar molecules (iodine), and large molecules (methylene
18 blue) [48]. Based on the optimization results of the experimental design, the SCG-AC is both
19 a microporous and mesoporous material. Therefore, it is suitable for the adsorption of small
20 and large molecules.

21 **Table 5. Optimization of SCG-AC by RSM**

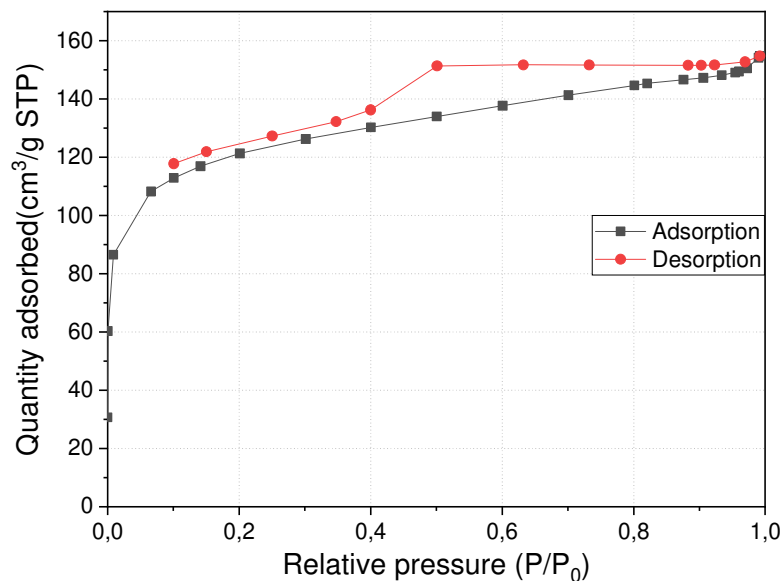
A: Acid concentration (wt%)	B: impregnation ratio	C: Temperature (°C)	Iodine number (mg/g)		error (%)	Methylene blue number (mg/g)		error (%)
			Pred	Exp		Pred	Exp	
68.70	1.50	500	1148	1139	0.80	87	90	3.45

22 **3.8. Characterization of the SCG-AC prepared under the optimal conditions**

1 The results of elemental analyzers for the optimal SCG-AC are presented in Table 6.
2 According to the elemental analysis, activated carbon derived from SCG contains 2.06 wt%
3 of nitrogen. Nitrogen is expected to be incorporated into the carbon matrix as a result of the
4 presence of caffeine in the organic precursor [26]. A significant amount of oxygen is also
5 detected due to the oxygen surface functional groups. The number of oxygen surface
6 functional groups is an imperative characteristic of the AC. The presence of oxygen
7 functional groups is essential to ensure the development of a high microporosity structure on
8 the AC [49]. Phosphorus species are not removed from the carbon surface and their content
9 reaches 6.84 wt%. According to the EDX data, the significant proportions of P, Ca and K can
10 affect the acidic and basic properties of the carbon surface and thus influence the adsorption
11 behavior [50]. In this respect, it was revealed that the existence of phosphorus in the carbon
12 matrix (due to the chemical activation by phosphoric acid) increases its capacity and
13 selectivity for the elimination of thiophene compounds. Indeed, these phosphorus species
14 have a strong acidity that enhances the attraction of thiophene compounds whose character is
15 slightly basic [51]. Thus the occurrence of these species on the surface of the SCG-AC
16 resulting the use of phosphoric acid as an activating agent can improve the adsorption of
17 thiophene [26,51].

18 The interaction between the hydrogen atoms of the carboxylic groups and the sulfur atom has
19 been proved to be favorable for the adsorption of sulfur compounds, thanks to the increase in
20 the adsorption energies involved for these molecules [16]. Hence the carboxylic functional
21 groups contribute favorably to the adsorption of sulfur molecules. Table 6 summarizes the
22 amount of acidic and basic groups obtained from Boehm's titration method. The surface of
23 the SCG-derived carbon is rich on acidic groups and more precisely on carboxylic groups
24 (0.32 mmol.g^{-1}). The acidic groups may be derived from the reaction between H_3PO_4 and
25 precursor material during the activation [17]. Whence the acidic nature of the SCG-AC. The

1 presence of oxygen-containing functional groups on the surface of the AC enhances the
2 exchanges between the SCG-AC and thiophene and then the enhancement of its elimination.
3 The point of zero charges is the pH at which the surface of an adsorbent is neutral. Thus, the
4 AC contains as much positively charged as negatively charged surface functions. The pH_{pzc} of
5 the optimized SCG-AC assert the dominance of the acidic groups on the AC surface. The
6 specific surface area (S_{BET}) of the SCG-derived carbon was determined from N_2 adsorption
7 isotherms (see Fig. 8). The plot of the optimal SCG-AC exhibits a typical hybrid type I-IV
8 isotherm. The observed hysteresis is due to the capillary condensation taking place in
9 mesopores, and the limiting uptake over a range of high P/P_0 [52]. The hysteresis can be
10 classified as type H2 according to the IUPAC classification. It was found that adsorbent that
11 gives rise to H2 hysteresis is often disordered and the distribution of pore size and shape is
12 not well defined [52]. The SCG-AC hysteresis loop is more pronounced than those founded
13 by Ramasahayam et al.[53] for the same precursor which is a result of pore propagation and
14 mesopores widening in the presence of the activating agent H_3PO_4 . An interesting observation
15 was also detected: the non-closure point of the desorption branch at low relative pressures.
16 This can be due to irreversible chemical interaction between N_2 and adsorbent [53]. The
17 results of the structural characterization of the SCG-AC sample by scanning electron
18 microscopy and X-Ray diffraction will be reported in future work. The S_{BET} and the total pore
19 volume are $410 \text{ m}^2/\text{g}$ and $0.25 \text{ cm}^3/\text{g}$ respectively. Similar results for the specific surface area
20 ($405.68 \text{ m}^2/\text{g}$) of the spent coffee grounds derived carbon prepared by chemical activation
21 with the ZnCl_2 were found by Yuliusman and al. [54].



1
2 **Fig. 8. N₂ adsorption-desorption isotherm of SCG-AC prepared at optimized conditions.**

3 **Table 6. Textural properties, surface functional groups, and pH_{pzc} values of the SCG-**
4 **AC prepared at optimized conditions.**

Element analysis (wt%)										
C	H	N	S	O	P	Cl	Ca	K	Cu	Fe
69.70	3.20	2.06	<LD	18.24	6.84	1.72	0.82	0.56	0.04	0.02
Acidic functional groups (mmol.g ⁻¹)										
carboxylic groups		phenolic groups		lactonic groups		total acidic groups		basic groups		pH _{pzc}
0.32		0.00		0.18		0.50		0.36		3.60
Textural properties										
S _{BET} (m ² /g)		Average pore diameter (nm)			V _T (cm ³ /g)		V _{mic} (cm ³ /g)		V _{meso} (cm ³ /g)	
410.00		2.44			0.25		0.05		0.04	

5 **3.9. Comparison with the iodine and methylene blue adsorption value of activated**
6 **carbon prepared from various lignocellulosic biomass**

7 A comparison study has been done between the iodine and methylene blue adsorption value
8 of the SCG-AC with those carbons obtained in the literature prepared from various
9 agricultural wastes is represented in Table 7. As is apparent from the table that the iodine and
10 methylene blue adsorption values of SCG-AC is relevant to other studies investigated by
11 other works. Thus this research revealed the usage of the spent coffee grounds as an

1 economical, accessible raw feedstock with great potential of producing activated carbon with
2 high iodine and methylene blue adsorption values.

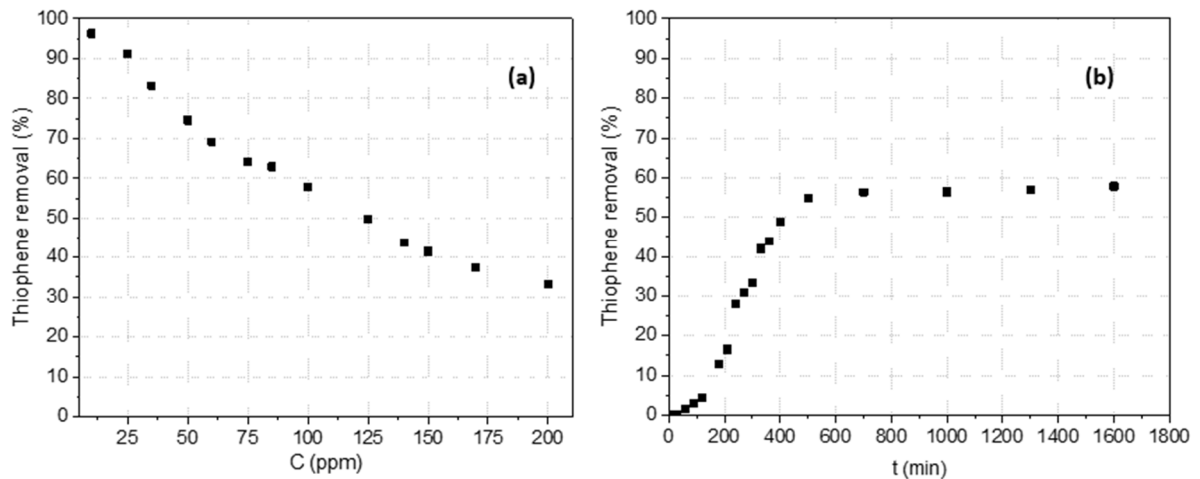
3 **Table 7. Comparison of the iodine and methylene blue adsorption value of activated**
4 **carbon prepared from various lignocellulosic biomass.**

Precursors	Activating agent	IN	MB	Ref
Pomegranate peels	H ₃ PO ₄	1455	168	[24]
Almond shells		791	148	[55]
Banana trunk		-	64.66	[22]
Cotton fabrics		595.21	-	[23]
Spent coffee grounds		1139	90	This work

5 **3.10. Adsorptive desulfurization**

6 **3.10.1. Effect of adsorbate dose and contact time on the adsorption efficiency of SCG-** 7 **AC**

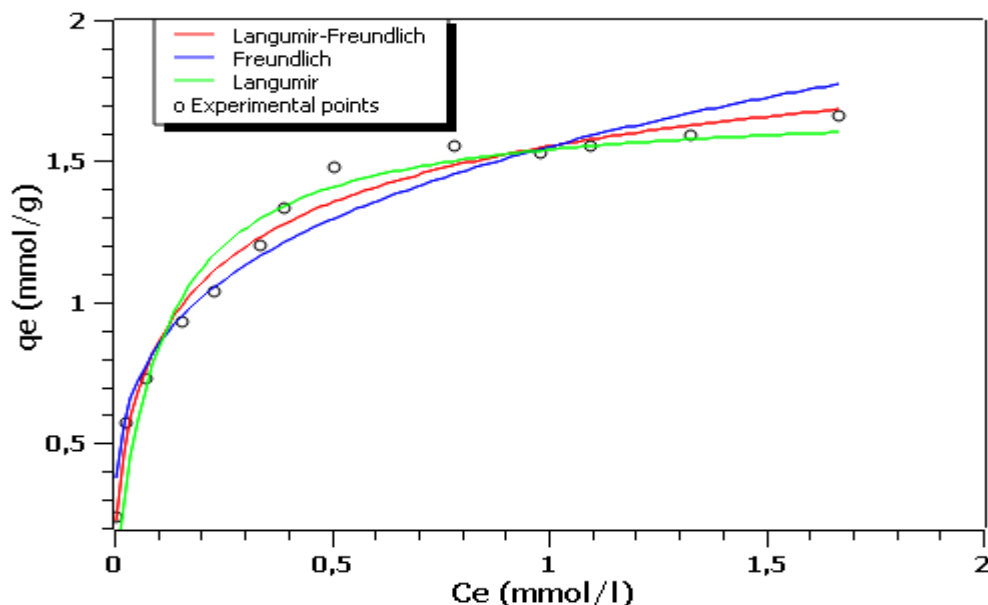
8 To assess the influence of adsorbate dose on the thiophene removal, different initial
9 concentrations of thiophene were used (Fig. 9a). We noticed that the increase of adsorbate
10 initial concentration led to the decrease in percent removal. The SCG-AC has achieved more
11 than 96% and 91% thiophene removal at concentrations of 10 ppm and 25 ppm, respectively
12 in 100 min. At extremely higher initial concentrations the thiophene removal efficiency of the
13 SCG-AC declined to 33 % removal at 200 ppm initial thiophene concentration. The influence
14 of residence time on the removal performance of the thiophene has also been investigated.
15 Adsorption was studied at various time intervals (0–1600 min) at a fixed initial concentration
16 of adsorbates (100 ppm). The obtained removal percentages were plotted against the
17 equilibrium time to show clearly the effect of contact time for kinetic modelling. Fig. 9b
18 reveals the impact of contact time on the elimination of thiophene by the SCG-AC. The
19 adsorption was fast within the first 500 min for thiophene but slowing down between 500 and
20 1600 min as equilibrium was attained. The adsorption capacity of thiophene was 57.80 %.



1 **Fig. 9. Effect of Adsorbate dose on the removal capacity of SCG-AC (b) Effect of contact**
 2 **time on the adsorption performance of SCG-AC.**
 3

4 **3.10.2. Isotherms of thiophene adsorption at ambient conditions**

5 The relationship between the adsorbed amount of thiophene and its equilibrium concentration
 6 at a constant temperature can be represented by an adsorption isotherm. The adsorption
 7 isotherm is the most employed method for representing the equilibrium state of an adsorption
 8 system. From Fig. 10, the adsorption capacity of thiophene (q_e) increases with the progression
 9 of the equilibrium concentration (C_e). Therefore, the equilibrium adsorption isotherm can be
 10 used to describe the interactivity behavior between the adsorbate and the adsorbent as well as
 11 the design of the adsorption system [5].



1
2 **Fig.10. Thiophene adsorption isotherms at 25 °C on the optimal SCG-AC**

3 The calculated adsorption capacities (from Fig. 10) are listed in Table 8. It is clear from the
4 coefficients of correlations (R^2) that the Langmuir–Freundlich isotherm fits the present data
5 much better than Langmuir and Freundlich isotherm. These results show that the Langmuir–
6 Freundlich isotherm represents the adsorption data of thiophene on SCG-AC in the range of
7 the studied concentration. **According to this model, the adsorption of a molecule is not done**
8 **on one adsorption site but on $1/n$ site.** This is reliable with the fact that Langmuir-Freundlich
9 isotherm is based on the hypothesis that an adsorbent has a highly heterogeneous surface with
10 different sites for adsorption or different functional groups.

11 **Table 8. The parameters of different isotherms for the adsorption of thiophene in gas**
12 **phase by SCG-AC**

Langmuir			Freundlich			Langmuir- Freundlich			
q_m (mmol/g)	K_L (l/mmol)	R^2	K_F $l^{1/n} \text{ mmol}^{(1-1/n)} \text{ g}^{-1}$	$1/n$	R^2	q_m (mmol/g)	K_{LF} (l/mmol)	$1/n$	R^2
1.70	9.44	0.9504	1.55	0.33	0.9582	2.23	4.07	0.56	0.9880

1 Due to the lack of data from the literature about the adsorption of thiophene in gas phase
 2 under ambient conditions, this work exposed a comparison with others reported results to
 3 know the capacity range of adsorption of thiophene by different adsorbents (Table 9).
 4 Although our SCG-AC provided a better adsorption capacity than other adsorbents from the
 5 works of Edinger et al. [3] and Prajapati et al. [56], however it still less performant than those
 6 of Ag-Y and Cu-Y [13]. This can be described by the variance in surface chemistry, textural
 7 properties as well as the bonding strength between the thiophene and the AC [57]. A
 8 comparative study with tetrahydrothiophene under the same operating conditions showed a
 9 close adsorption capacity between SCG-AC and the Fiber-cloth material (ACFC).

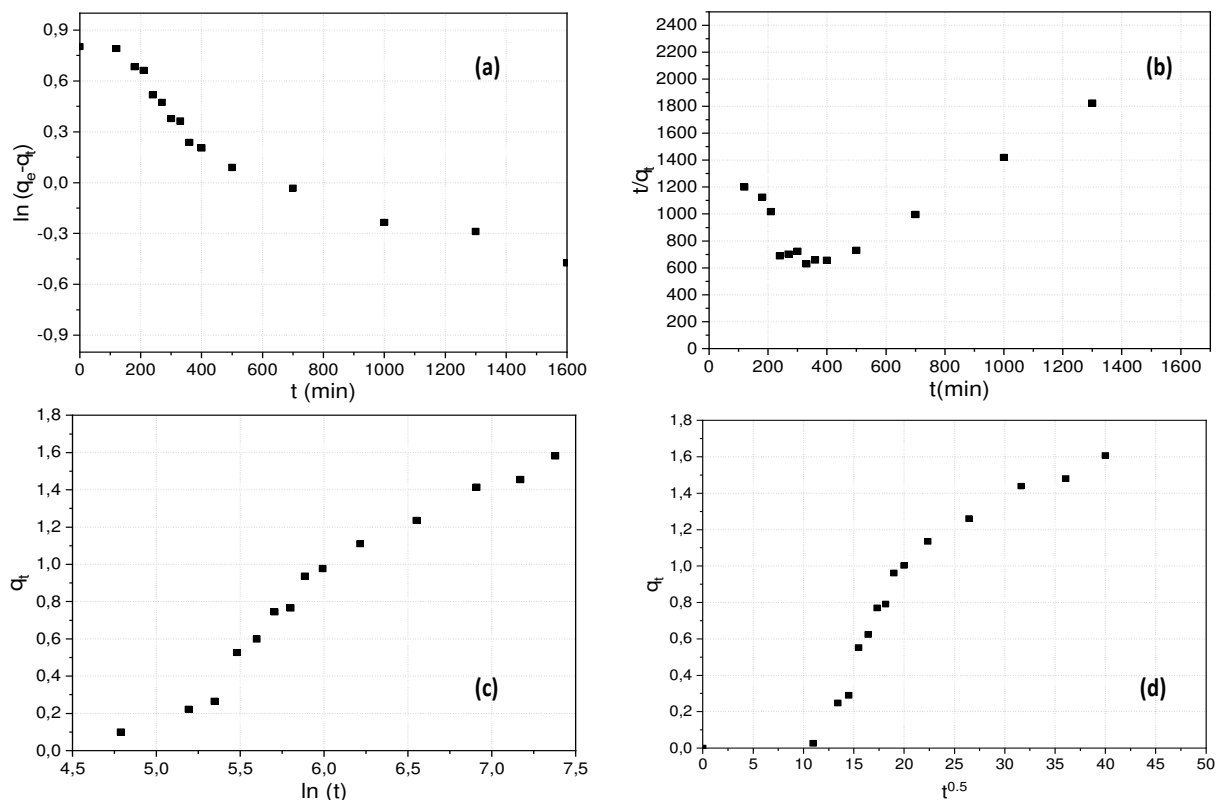
10 **Table 9. Uptake gas desulfurization capacity of different adsorbent materials**

Adsorbents	Conditions	Adsorbate	Temperature (°C)	Adsorbent capacity (mmol/g)	References
Ag-Y	Dynamic gas phase	Thiophene	180	2.602	[13]
Cu-Y			90	3.910	
Na-ZSM5			90	1.023	
Commercial AC			100	0.138	[3]
Ni/Cu dispersed carbon nanofiber			150	0.006	[56]
Fiber-cloth material (ACFC)	Static gas phase	Tetrahydrothiophene	25	2.300	[57]
SCG-AC	Static gas phase	Thiophene	25	2.230	Present study

11 **3.10.3. Kinetic of thiophene adsorption**

12 Kinetic studies and isotherm models are a used tools to simulate and describe experimental
 13 equilibrium data of an adsorption process [33]. Experimental data were fitted with kinetic
 14 models and the results were presented in Fig. 11(a, b, c). The adsorption kinetics are analyzed
 15 according to the pseudo-first-order model (equation 7) pseudo-second-order (equation 8), and
 16 Elovich model (equation 9). The results of the kinetic parameters were collected in Table 10.

1 The applicability of pseudo-first-order, pseudo-second-order, and Elovich models to the
 2 kinetics of thiophene sorption by SCG-AC were evaluated by comparing the value of the
 3 correlation coefficients, R^2 . The best kinetic model describing the thiophene adsorption was
 4 the Elovich model ($R^2=0.9507$). The Elovich model is a well-known model that described the
 5 adsorption of gas onto solid systems [33]. This means that the rate limiting step in the process
 6 is the chemical sorption between the thiophene and the active sites of the SCG-AC.
 7 According to the Elovich model assumptions, there are probably two types of sorption sites
 8 implying in this sorption process. One with the oxygen surface groups by complexation and
 9 the other one with the π electrons of the graphene layers of the activated carbon
 10 by electrostatic interaction [58].



11 **Fig. 11. Plots of pseudo-first order kinetic (a) pseudo-second order adsorption kinetic**
 12 **(b), Elovich model (c) and intraparticle diffusion (d) for the adsorption of thiophene**
 13 **at initial concentration of 100 ppm and mSCG-AC=1g.**
 14

15
 16

1

2

Table 10. Kinetic parameters obtained for thiophene adsorption on SCG-AC.

	SCG-AC
$q_{e, \text{exp}}$ (mmol g ⁻¹)	1.65
Pseudo-first-order	
q_e (mmol g ⁻¹)	1.99
K_1 (min ⁻¹)	0.80×10^{-3}
R^2	0.8893
Pseudo-second-order	
q_e (mmol g ⁻¹)	0.77
K_2 (g mmol ⁻¹ min ⁻¹)	3.80×10^{-3}
R^2	0.7920
Elovich model	
β (mmol g ⁻¹)	1.63
α (mmol g ⁻¹ min ⁻¹)	6.19×10^{-3}
R^2	0.9507

3

3.10.4. Adsorption mechanism

5 The influence of mass transfer resistance on binding of thiophene on the SCG-AC was

6 verified by exploring Weber and Morris intra-particle diffusion resistance model using

7 equation 10. According to the intraparticle diffusion model, the curve representing the amount

8 adsorbed as a function of $t^{1/2}$ must be linear and pass through the origin if the intraparticle

9 diffusion is involved in the adsorption process. In this case, intraparticle diffusion should be

10 the step that controls the adsorption rate [1]. In our case, the deviation of the line of the

11 intraparticle diffusion model from the origin represents the effect of the diffusion through the

12 film surrounding the particles of the SCG-AC. The greater the deviation, the more significant

13 will be the effect of the mass transfer in the film on the kinetics of the adsorption process

14 [59]. The Table 11 illustrates the intra-particle diffusion model parameters. We note that the

15 representative line of the model (Fig. 11d) does not go through the origin and that the

16 correlation coefficient ($R^2=0.8768$) is weak. This result shows that intraparticle diffusion is

17 not the only rate-controlling phase [37]. Therefore, the adsorption proceeds via a complex

18 mechanism consisting of both kinetic and intra-particle transport within the pores of adsorbent

[59]. This is supported by a finding shown in Fig. 12 where the adsorption of thiophene occurred in two phases: rapid and slow phases. This is due to the great availability of vacant active sites on the SCG-AC surface. As the time increased slower step took place where the active sites on which thiophene binds become fewer. The formation of monolayer of thiophene at the exterior surface became saturated as the amount of thiophene molecules was higher than the available sites (see Fig. 12). The saturation of thiophene forced the system to prevent the changes in order to remain in equilibrium state which also contributed to a slow phase [33].

Table 11. Intra-particle diffusion parameters for adsorption of thiophene

	K_{id} ($\text{mmol g}^{-1} \text{min}^{-0.5}$)	C (cal)	R^2
SCG-AC	48.2×10^{-3}	-0.15	0.8768

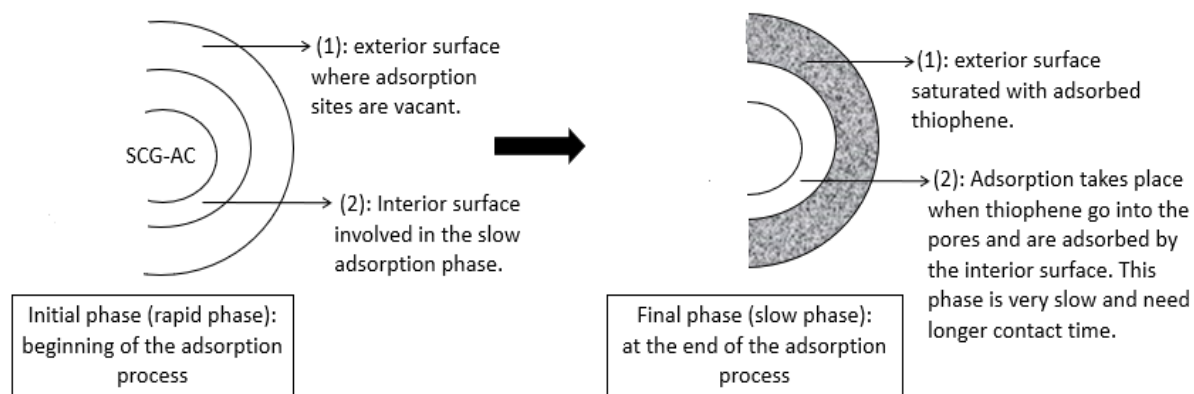


Fig. 12. Schematic diagram of thiophene adsorption process on the SCG-AC.

Conclusions

The AC prepared from SCG by chemical activation with H_3PO_4 was optimized using RSM. Process optimization of SCG-based AC was successfully explored by BBD of RSM. The ANOVA of the primary factors indicated that the impregnation ratio and acid concentration have the most significant effect on the iodine adsorption, whereas the acid concentration, impregnation ratio, and activation temperature have the most substantial impact on the methylene blue adsorption. The optimal conditions for maximum iodine and methylene blue adsorption have been found for an activation temperature of $500\text{ }^\circ\text{C}$ with an impregnation

1 ratio of 1.5 g/g, and phosphoric acid concentration of 68.7 wt%. The Boehm results confirm
2 that carboxylic acids are the main functional groups found on the surface of the optimal SCG-
3 AC. The nitrogen adsorption-desorption isotherms of the **produced material exhibit a typical**
4 **hybrid type I-IV isotherm with hysteresis type H2** and the BET surface area was 410 m²/g.
5 The optimized SCG-AC was **used in adsorptive desulfurization** of thiophene from the gas at
6 ambient temperature. A good agreement between experimental results and Langmuir–
7 Freundlich isotherm was obtained. **According to this model, the adsorption of thiophene takes**
8 **place via 1/ n site. The best kinetic model describing the thiophene adsorption was the**
9 **Elovich model which suggests that there are probably two types of sorption sites implying in**
10 **this sorption process: one with the oxygen surface groups by complexation and the other one**
11 **with the π electrons of the graphene layers of the activated carbon by electrostatic interaction.**
12 **According to the proposed mechanism, the adsorption of thiophene on the SCG-AC proceeds**
13 **via a complex mechanism consisting of both kinetic and intra-particle transport within the**
14 **pores of the adsorbent. This study was established in order to get first trends about the**
15 **adsorption capacities of activated carbon prepared from spent coffee grounds, towards**
16 **thiophene adsorption. Though reported sorption capacities are promising, experiments were**
17 **performed at ambient conditions while the envisaged application of SCG-AC in fluidized**
18 **catalytic cracking (FCC) gasoline treatment demands elevated ones (around 500 °C). The**
19 **effect of temperature will be the subject of future work.**

20

21 **Acknowledgements**

22 This work has been partly carried-out in the frame of the Partenariat Hubert Curien Program
23 through the PHC UTIQUE 2017 (Project code: 17G1139) and the authors gratefully
24 acknowledge the support of the Comité Mixte Franco-Tunisien (CMCU) and the University

1 of Gabes (Tunisia). The authors are grateful to Mr. Eric CHEVREL of IMT Atlantique for his
2 assistance in the activated carbon production tests.

1 **References**

- 2 [1] T.A. Saleh, K.O. Sulaiman, S.A. AL-Hammadi, H. Dafalla, G.I. Danmaliki, Adsorptive
3 desulfurization of thiophene, benzothiophene and dibenzothiophene over activated
4 carbon manganese oxide nanocomposite: with column system evaluation, *J. Clean. Prod.*
5 154 (2017) 401–412.
- 6 [2] B. Li, W. Guo, S. Yuan, J. Hu, J. Wang, H. Jiao, A theoretical investigation into the
7 thiophene-cracking mechanism over pure Brønsted acidic zeolites, *J. Catal.* 253 (2008)
8 212–220.
- 9 [3] P. Edinger, D. Grimekis, K. Panopoulos, S. Karellas, C. Ludwig, Adsorption of
10 thiophene by activated carbon: A global sensitivity analysis, *J. Environ. Chem. Eng.* 5
11 (2017) 4173–4184.
- 12 [4] M.A. Betiha, A.M. Rabie, H.S. Ahmed, A.A. Abdelrahman, M.F. El-Shahat, Oxidative
13 desulfurization using graphene and its composites for fuel containing thiophene and its
14 derivatives: An update review, *Egypt. J. Pet.* (2017).
- 15 [5] T. Nunthaprechachan, S. Pengpanich, M. Hunsom, Adsorptive desulfurization of
16 dibenzothiophene by sewage sludge-derived activated carbon, *Chem. Eng. J.* 228 (2013)
17 263–271.
- 18 [6] R. Liu, Y. Zhang, J. Ding, R. Wang, M. Yu, Ion exchange resin immobilised 12-
19 tungstophosphoric acid as an efficient and recoverable catalyst for the oxidative removal
20 of organosulfur targeting at clean fuel, *Sep. Purif. Technol.* 174 (2017) 84–88.
- 21 [7] F. Subhan, S. Aslam, Z. Yan, M. Ikram, S. Rehman, Enhanced desulfurization
22 characteristics of Cu-KIT-6 for thiophene, *Microporous Mesoporous Mater.* 199 (2014)
23 108–116.

- 1 [8] B. Pawelec, R. M. Navarro, J. Miguel Campos-Martin, J.L. G. Fierro, Retracted article:
2 Towards near zero- sulfur liquid fuels : a perspective review, Catal. Sci. Technol. 1
3 (2011) 23–42.
- 4 [9] M. Aslam Abdullah, N. Rao, A. Singh, NOVEL METHODS OF DEEP
5 DESULFURIZATION: A REVIEW., Pet. Coal. 61 (2019).
- 6 [10] M.A. Safa, R. Al-Majren, T. Al-Shamary, J.-Il. Park, X. Ma, Removal of sulfone
7 compounds formed in oxidative desulfurization of middle distillate, Fuel. 194 (2017)
8 123–128.
- 9 [11] F.A. Duarte, P. de A. Mello, C.A. Bizzi, M.A. Nunes, E.M. Moreira, M.S. Alencar, H.N.
10 Motta, V.L. Dressler, É.M. Flores, Sulfur removal from hydrotreated petroleum fractions
11 using ultrasound-assisted oxidative desulfurization process, Fuel. 90 (2011) 2158–2164.
- 12 [12] A. Shawky, R.M. Mohamed, I.A. Mkhaldid, N.S. Awwad, H.A. Ibrahim, One-pot
13 synthesis of Mn₃O₄-coupled Ag₂WO₄ nanocomposite photocatalyst for enhanced
14 photooxidative desulfurization of thiophene under visible light irradiation, Appl.
15 Nanosci. (2019).
- 16 [13] A. Takahashi, F.H. Yang, R.T. Yang, New Sorbents for Desulfurization by π -
17 Complexation: Thiophene/Benzene Adsorption, Ind. Eng. Chem. Res. 41 (2002) 2487–
18 2496.
- 19 [14] S. Xun, W. Zhu, D. Zheng, L. Zhang, H. Liu, S. Yin, M. Zhang, H. Li, Synthesis of
20 metal-based ionic liquid supported catalyst and its application in catalytic oxidative
21 desulfurization of fuels, Fuel. 136 (2014) 358–365.
- 22 [15] Y. Shi, X. Zhang, L. Wang, G. Liu, MOF-derived porous carbon for adsorptive
23 desulfurization, AIChE J. 60 (2014) 2747–2751.

- 1 [16] C. Yu, J.S. Qiu, Y.F. Sun, X.H. Li, G. Chen, Z.B. Zhao, Adsorption removal of
2 thiophene and dibenzothiophene from oils with activated carbon as adsorbent: effect of
3 surface chemistry, *J. Porous Mater.* 15 (2008) 151–157.
- 4 [17] T. Mahmood, R. Ali, A. Naeem, M. Hamayun, M. Aslam, Potential of used *Camellia*
5 *sinensis* leaves as precursor for activated carbon preparation by chemical activation with
6 H₃PO₄; optimization using response surface methodology, *Process Saf. Environ. Prot.*
7 109 (2017) 548–563.
- 8 [18] M.A. Bezerra, R.E. Santelli, E.P. Oliveira, L.S. Villar, L.A. Escaleira, Response surface
9 methodology (RSM) as a tool for optimization in analytical chemistry, *Talanta.* 76
10 (2008) 965–977.
- 11 [19] S. Das, S. Mishra, Box-Behnken statistical design to optimize preparation of activated
12 carbon from *Limonia acidissima* shell with desirability approach, *J. Environ. Chem.*
13 *Eng.* 5 (2017) 588–600.
- 14 [20] A.I. Khuri, S. Mukhopadhyay, Response surface methodology, *Wiley Interdiscip. Rev.*
15 *Comput. Stat.* 2 (2010) 128–149.
- 16 [21] S. Choojit, C. Sangwichien, PREPARATION OF ACTIVATED CARBON
17 PRODUCTION FROM OIL PALM EMPTY FRUIT BUNCH AND ITS
18 APPLICATION, (2018) 20.
- 19 [22] M. Danish, T. Ahmad, W.N.A.W. Nadhari, M. Ahmad, W.A. Khanday, L. Ziyang, Z.
20 Pin, Optimization of banana trunk-activated carbon production for methylene blue-
21 contaminated water treatment, *Appl. Water Sci.* 8 (2018) 9.
- 22 [23] R. Salehi, F. Dadashian, M. Abedi, B. Hasani, Optimization of chemical activation of
23 cotton fabrics for activated carbon fabrics production using response surface
24 methodology, *J. Text. Inst.* 109 (2018) 1586–1594.

- 1 [24] T. Senthilkumar, S.K. Chattopadhyay, L.R. Miranda, Optimization of Activated Carbon
2 Preparation from Pomegranate Peel (*Punica granatum* Peel) Using RSM, Chem. Eng.
3 Commun. 204 (2017) 238–248.
- 4 [25] Yuliusman, Nasruddin, M.K. Afdhol, F. Haris, R.A. Amiliana, A. Hanafi, I.T.
5 Ramadhan, Production of Activated Carbon from Coffee Grounds Using Chemical and
6 Physical Activation Method, (2017).
- 7 [26] K. Kante, C. Nieto-Delgado, J.R. Rangel-Mendez, T.J. Badosz, Spent coffee-based
8 activated carbon: Specific surface features and their importance for H₂S separation
9 process, J. Hazard. Mater. 201–202 (2012) 141–147.
- 10 [27] B. Li, W. Guo, S. Yuan, J. Hu, J. Wang, H. Jiao, A theoretical investigation into the
11 thiophene-cracking mechanism over pure Brønsted acidic zeolites, J. Catal. 253 (2008)
12 212–220.
- 13 [28] P. Baeza, G. Aguila, G. Vargas, J. Ojeda, P. Araya, Adsorption of thiophene and
14 dibenzothiophene on highly dispersed Cu/ZrO₂ adsorbents, Appl. Catal. B Environ. 111
15 (2012) 133–140.
- 16 [29] H.N. Tran, H.-P. Chao, S.-J. You, Activated carbons from golden shower upon different
17 chemical activation methods: synthesis and characterizations, Adsorpt. Sci. Technol. 36
18 (2018) 95–113.
- 19 [30] F. Bouhamed, Z. Elouear, J. Bouzid, Adsorptive removal of copper(II) from aqueous
20 solutions on activated carbon prepared from Tunisian date stones: Equilibrium, kinetics
21 and thermodynamics, J. Taiwan Inst. Chem. Eng. 43 (2012) 741–749.
- 22 [31] H.P. Boehm, Surface oxides on carbon and their analysis: a critical assessment, Carbon.
23 40 (2002) 145–149.
- 24 [32] A. Machrouhi, H. Alilou, M. Farnane, S. El Hamidi, M. Sadiq, M. Abdennouri, H.
25 Tounsadi, N. Barka, Statistical optimization of activated carbon from Thapsia

- 1 transtagana stems and dyes removal efficiency using central composite design, *J. Sci.*
2 *Adv. Mater. Devices.* 4 (2019) 544–553.
- 3 [33] N.R. Abdul Manap, R. Shamsudin, M.N. Maghpor, M.A. Abdul Hamid, A. Jalar,
4 Adsorption isotherm and kinetic study of gas-solid system of formaldehyde on oil palm
5 mesocarp bio-char: Pyrolysis effect, *J. Environ. Chem. Eng.* 6 (2018) 970–983.
- 6 [34] I. Langmuir, THE CONSTITUTION AND FUNDAMENTAL PROPERTIES OF
7 SOLIDS AND LIQUIDS. PART I. SOLIDS., *J. Am. Chem. Soc.* 38 (1916) 2221–2295.
- 8 [35] R.N. Fallah, S. Azizian, G. Reggers, R. Carleer, S. Schreurs, J. Ahenach, V. Meynen, J.
9 Yperman, Effect of aromatics on the adsorption of thiophenic sulfur compounds from
10 model diesel fuel by activated carbon cloth, *Fuel Process. Technol.* 119 (2014) 278–285.
- 11 [36] G.P. Jeppu, T.P. Clement, A modified Langmuir-Freundlich isotherm model for
12 simulating pH-dependent adsorption effects, *J. Contam. Hydrol.* 129 (2012) 46–53.
- 13 [37] T.A. Saleh, G.I. Danmaliki, Adsorptive desulfurization of dibenzothiophene from fuels
14 by rubber tyres-derived carbons: Kinetics and isotherms evaluation, *Process Saf.*
15 *Environ. Prot.* 102 (2016) 9–19.
- 16 [38] Y.S. Ho, G. McKay, Pseudo-second order model for sorption processes, *Process*
17 *Biochem.* 34 (1999) 451–465.
- 18 [39] W.J. Weber, J.C. Morris, Kinetics of Adsorption on Carbon from Solution, *J. Sanit. Eng.*
19 *Div.* 89 (1963) 31–60.
- 20 [40] J. Feroso, O. Mašek, Thermochemical decomposition of coffee ground residues by
21 TG-MS: A kinetic study, *J. Anal. Appl. Pyrolysis.* 130 (2018) 358–367.
- 22 [41] I.-Y. Eom, J.-Y. Kim, T.-S. Kim, S.-M. Lee, D. Choi, I.-G. Choi, J.-W. Choi, Effect of
23 essential inorganic metals on primary thermal degradation of lignocellulosic biomass,
24 *Bioresour. Technol.* 104 (2012) 687–694.

- 1 [42] S.V. Vassilev, C.G. Vassileva, Y.-C. Song, W.-Y. Li, J. Feng, Ash contents and ash-
2 forming elements of biomass and their significance for solid biofuel combustion, *Fuel*.
3 208 (2017) 377–409.
- 4 [43] G. Hotová, V. Slovák, O.S.G.P. Soares, J.L. Figueiredo, M.F.R. Pereira, Oxygen surface
5 groups analysis of carbonaceous samples pyrolysed at low temperature, *Carbon*. 134
6 (2018) 255–263.
- 7 [44] A. Machrouhi, H. Alilou, M. Farnane, S. El Hamidi, M. Sadiq, M. Abdennouri, H.
8 Tounsadi, N. Barka, Statistical optimization of activated carbon from *Thapsia*
9 *transtagana* stems and dyes removal efficiency using central composite design, *J. Sci.*
10 *Adv. Mater. Devices*. 4 (2019) 544–553.
- 11 [45] Z. Hajamini, M.A. Sobati, S. Shahhosseini, B. Ghobadian, Waste fish oil (WFO)
12 esterification catalyzed by sulfonated activated carbon under ultrasound irradiation,
13 *Appl. Therm. Eng.* 94 (2016) 141–150.
- 14 [46] M. Molina-Sabio, F. Rodríguez-Reinoso, Role of chemical activation in the development
15 of carbon porosity, *Colloids Surf. Physicochem. Eng. Asp.* 241 (2004) 15–25.
- 16 [47] N. Md-Desa, Z.A. Ghani, S. Abdul-Talib, C. Tay, OPTIMIZATION OF ACTIVATED
17 CARBON PREPARATION FROM SPENT MUSHROOM FARMING WASTE
18 (SMFW) VIA BOX-BEHNKEN DESIGN OF RESPONSE SURFACE
19 METHODOLOGY, *Malays. J. Anal. Sci.* 20 (2016) 461–468.
- 20 [48] Z. Jiang, Y. Liu, X. Sun, F. Tian, F. Sun, C. Liang, W. You, C. Han, C. Li, Activated
21 carbons chemically modified by concentrated H₂SO₄ for the adsorption of the pollutants
22 from wastewater and the dibenzothiophene from fuel oils, *Langmuir*. 19 (2003) 731–
23 736.
- 24 [49] Y.N. Chaiw, K.K. Ang, T. Lee, X.Y. Lim, INVESTIGATION OF THE COFFEE
25 WASTE-DERIVED ADSORBENT, *J. Eng. Sci. Technol.* (2016) 16.

- 1 [50] L.G. Sorokhaibam, V.M. Bhandari, M.S. Salvi, S. Jain, S.D. Hadawale, V.V. Ranade,
2 Development of Newer Adsorbents: Activated Carbons Derived from Carbonized *Cassia*
3 *fistula*, Ind. Eng. Chem. Res. 54 (2015) 11844–11857.
- 4 [51] M. Seredych, C.T. Wu, P. Brender, C.O. Ania, C. Vix-Guterl, T.J. Bandosz, Role of
5 phosphorus in carbon matrix in desulfurization of diesel fuel using adsorption process,
6 Fuel. 92 (2012) 318–326.
- 7 [52] K.S.W. Sing, Reporting physisorption data for gas/solid systems with special reference
8 to the determination of surface area and porosity (Provisional), Pure Appl. Chem. 54
9 (1982) 2201–2218.
- 10 [53] S.K. Ramasahayam, A.L. Clark, Z. Hicks, T. Viswanathan, Spent coffee grounds derived
11 P, N co-doped C as electrocatalyst for supercapacitor applications, Electrochimica Acta.
12 168 (2015) 414–422.
- 13 [54] Yuliusman, Nasruddin, M.K. Afdhol, F. Haris, R.A. Amiliana, A. Hanafi, I.T.
14 Ramadhan, Production of Activated Carbon from Coffee Grounds Using Chemical and
15 Physical Activation Method, Adv. Sci. Lett. 23 (2017) 5751–5755.
- 16 [55] M.S. İzgi, C. Saka, O. Baytar, G. Saraçoğlu, Ö. Şahin, Preparation and Characterization
17 of Activated Carbon from Microwave and Conventional Heated Almond Shells Using
18 Phosphoric Acid Activation, Anal. Lett. 52 (2019) 772–789.
- 19 [56] Y.N. Prajapati, N. Verma, Fixed bed adsorptive desulfurization of thiophene over Cu/Ni-
20 dispersed carbon nanofiber, Fuel. 216 (2018) 381–389.
- 21 [57] B. Boulinguez, P. Le Cloirec, Adsorption/Desorption of Tetrahydrothiophene from
22 Natural Gas onto Granular and Fiber-Cloth Activated Carbon for Fuel Cell Applications,
23 Energy Fuels. 23 (2009) 912–919.

- 1 [58] L. Largette, R. Pasquier, A review of the kinetics adsorption models and their application
2 to the adsorption of lead by an activated carbon, *Chem. Eng. Res. Des.* 109 (2016) 495–
3 504.
- 4 [59] Adsorptive desulphurization of model oil by Ag nanoparticles-modified activated carbon
5 prepared from brewer's spent grains, *J. Environ. Chem. Eng.* 5 (2017) 147–159.
6